

Aquifer Elevations and Representations in the San Mateo Study Area and Vicinity

Jesse Sprague

5/19/10

To visualize the slopes and gradients of the surface of each aquifer group, I have created a Triangulated Irregular Network (TIN) and a simple spherical Kriging model for each formation or Aquifer.

Although there is data for the Kg formation (Cretaceous – Gallup Sand Stone) there is only one data point with water surface elevation information therefore I have not created any surface models for this unit. Lack of data also has caused omission of a Kriging analysis on the Cretaceous Mancos Shale (Km) and complete omission of the Cretaceous Dilco or Dalton member (Kcda) with only two elevation data points.

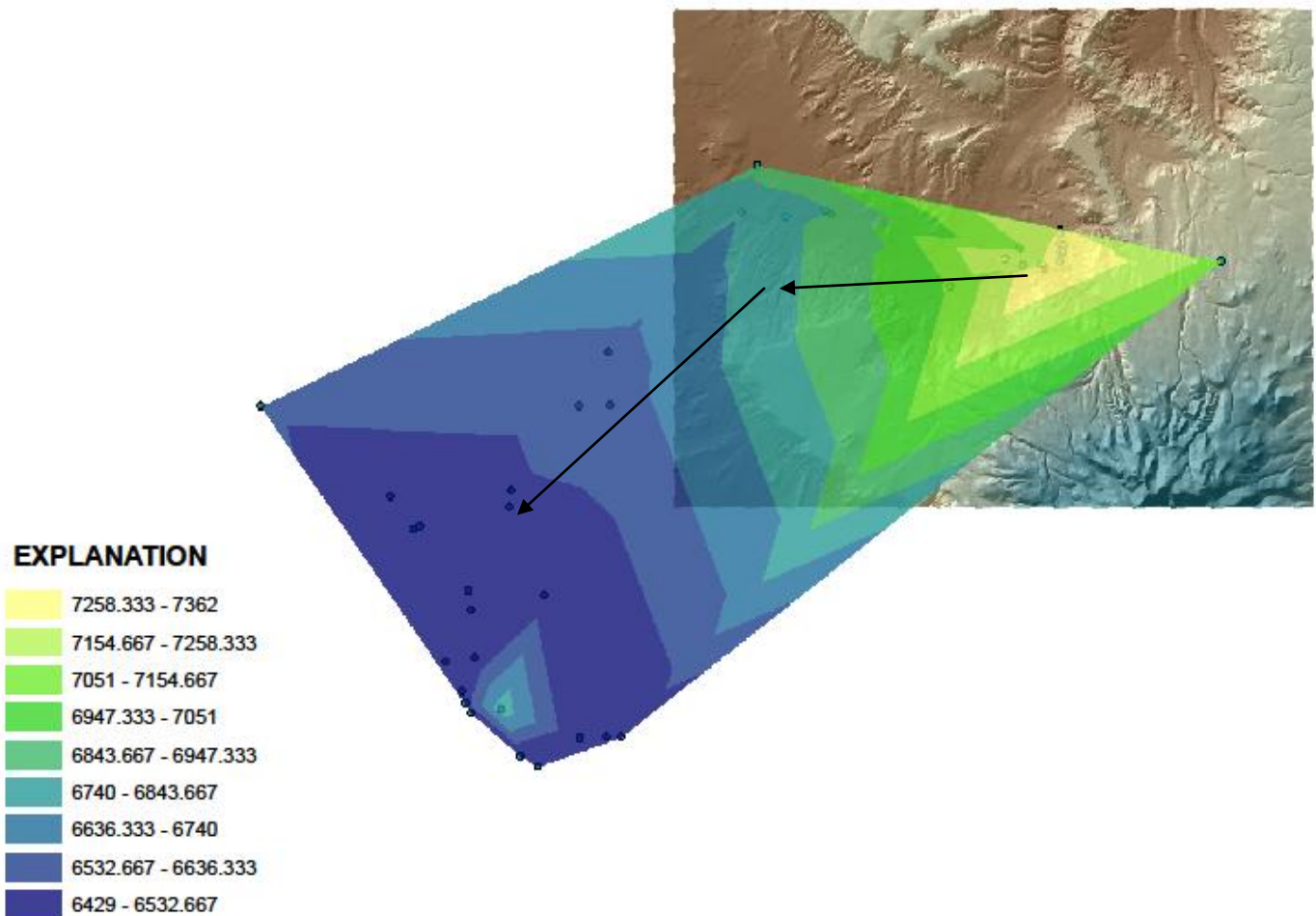
I will begin with upper formations and describe the flow directions of each aquifer with arrows added onto the images from ArcMap.

To generate these images I created Excel spread sheets with location information in Decimal Degrees - Lat/Long format. I then plotted the well locations in ArcMap and created TIN and Kriging analysis from the linked elevation data in each spread sheet.

Data sources are USGS, WATERS and RHR from Jeff Langman (USGS and WATERS) and Dan Kapostacy (RHR)

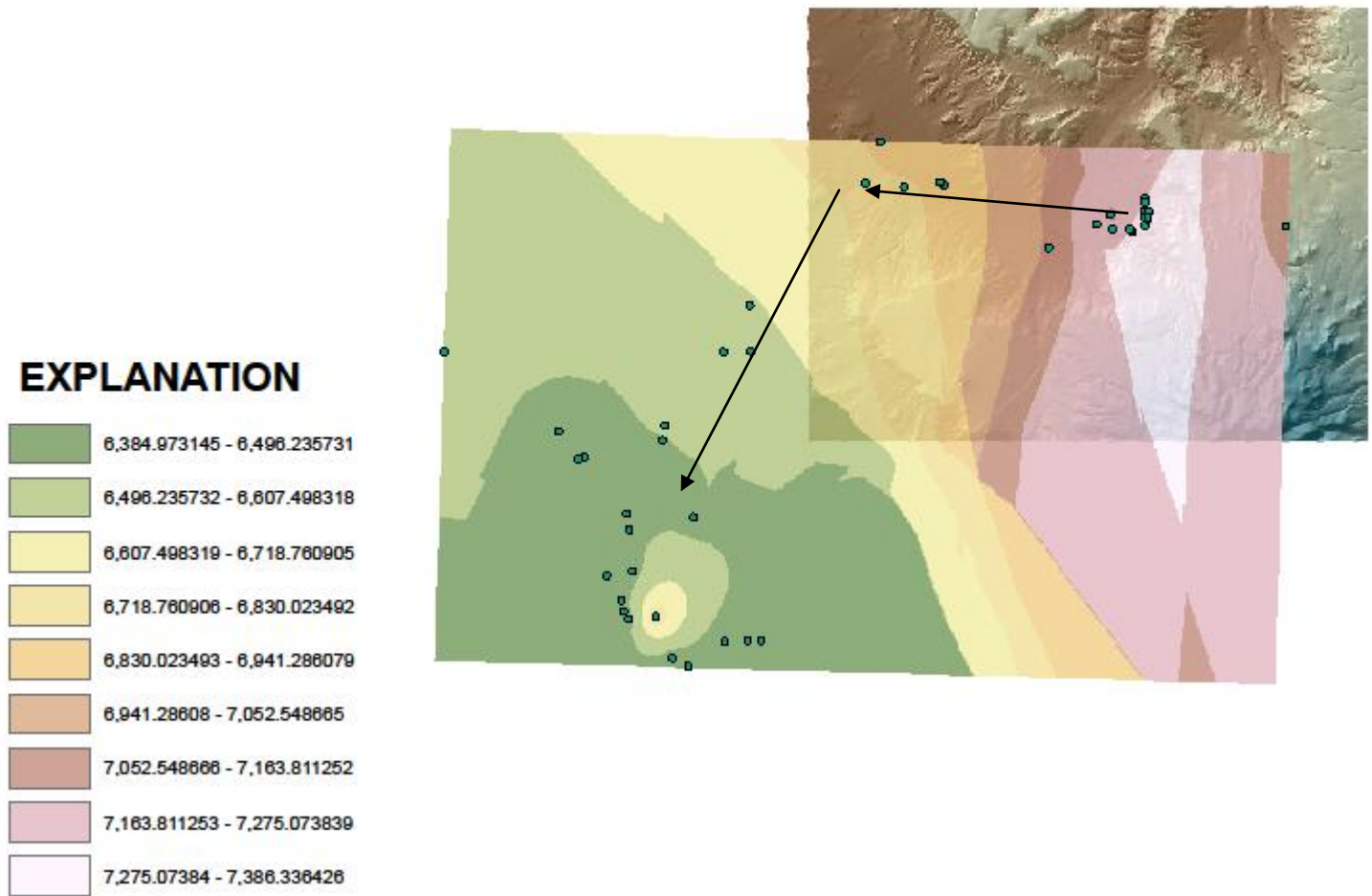
Potential mixing of aquifers was to be determined from a horizontal or side view of the TINs plotted together however because a TIN only shows probable potentiometric surfaces, areas with no overlap could still possibly be in a mixing region below the surface of the overlying aquifer.

Quaternary Aluvium TIN



This TIN Shows Quaternary Alluvial (Qal) Groundwater flowing out of the San Mateo Basin in a generally SW direction, what is not represented here is the flow interference from structural anomalies related to laramide or similar deformation (La Jara Mesa and associated Faults). This probably means the water is flowing in a azimuth similar to the San Mateo Creek that also exits the basin in a WSW direction shifting SW after it rounds La Jara Mesa. This TIN can support this hypothesis. An anomalous peak in the southern portion of the Alluvium Aquifer is noticeable in this figure, possibly extraneous as it is a single outlier causing the distortion among several other very similar results.

Quaternary Aluvium Kriging



A Kriging analysis of the same data supports the suggestion that a change in direction of flow of Alluvial groundwater is probable, the elevation gradients here are determined with a spatial correlation equation giving importance to closer objects generating a representation of the surface of the aquifer that further supports the hypothesis that groundwater direction changes in the Alluvial Aquifer to the South and West of the study area.

Again, if the outlying peak is ignored a perfect gradient is preserved.

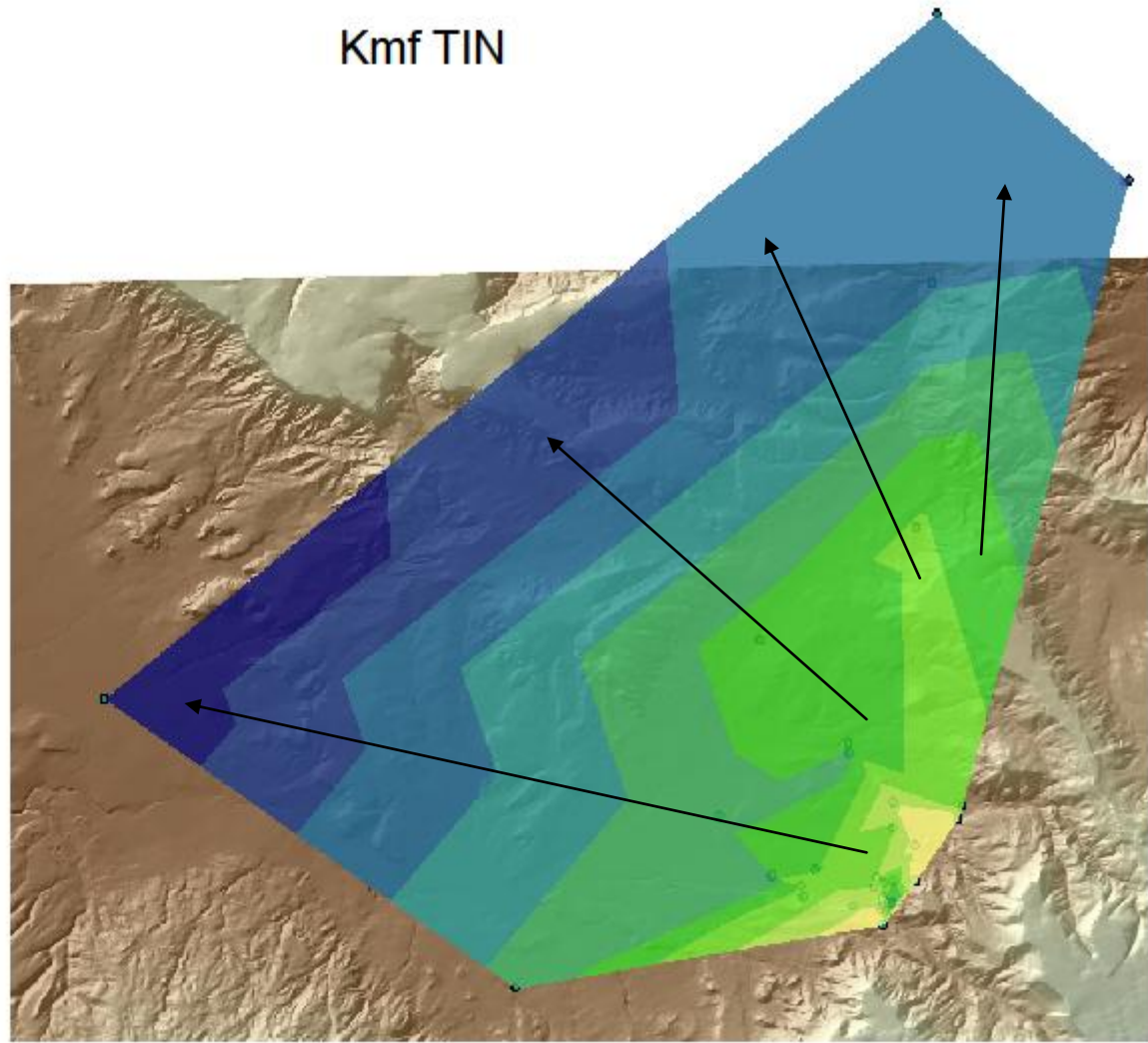
Below the Quaternary Aquifer is the Cretaceous Menifee (Kmf) aquifer which in many places is probably safe to consider the same aquifer as the Quaternary due to the geology of the region. The most notable difference in these aquifers is, for the purpose of this report, location. The Kmf aquifer samples are all generally taken from the eastern side of the San Mateo Basin, where the Qal tends to be sampled to the West.

Kmf TIN

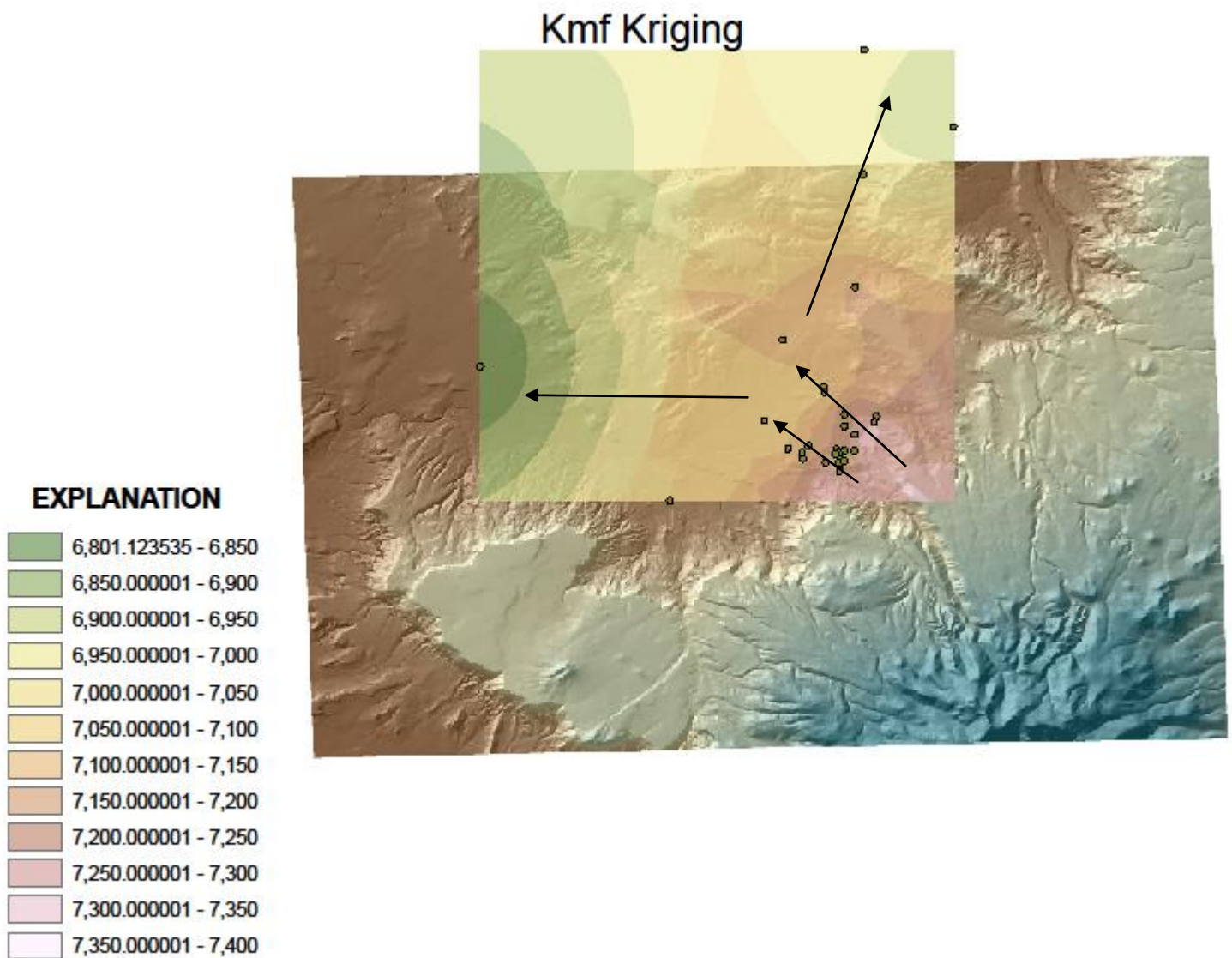
EXPLANATION

Elevation (ft)

7264.789 - 7323
7206.578 - 7264.789
7148.367 - 7206.578
7090.156 - 7148.367
7031.944 - 7090.156
6973.733 - 7031.944
6915.522 - 6973.733
6857.311 - 6915.522
6799.1 - 6857.311



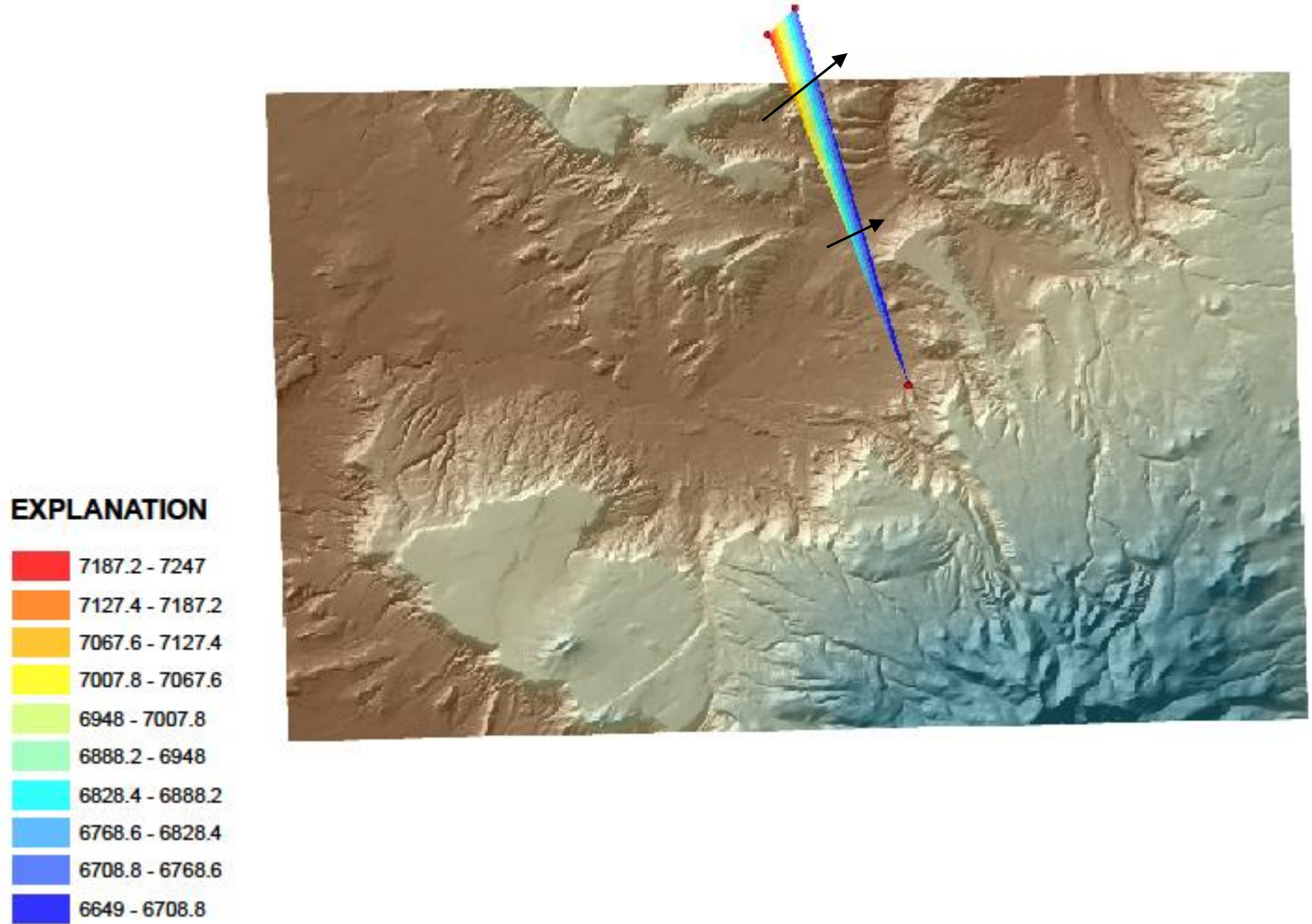
The TIN for the Meniffee aquifer shows down gradient directions sloping away from the base of Mt. Taylor. No anomalous elevations in this data set are obvious, and the flow direction represents what is expected as well as concurring with the TIN.



A Kriging analysis of the same data shows a plateau in the surface of the aquifer, before either dropping to the west in the San Mateo Basin or being distributed to the north outside of the study area.

A lack of data points for the Cretaceous Mancos Shale (Km) caused a poor Kriging analysis and generated no discernable results however a TIN was able to depict some slope gradient for the aquifer surface. The Data available suggest drainage to the NW as expected in the San Mateo Report.

Km TIN



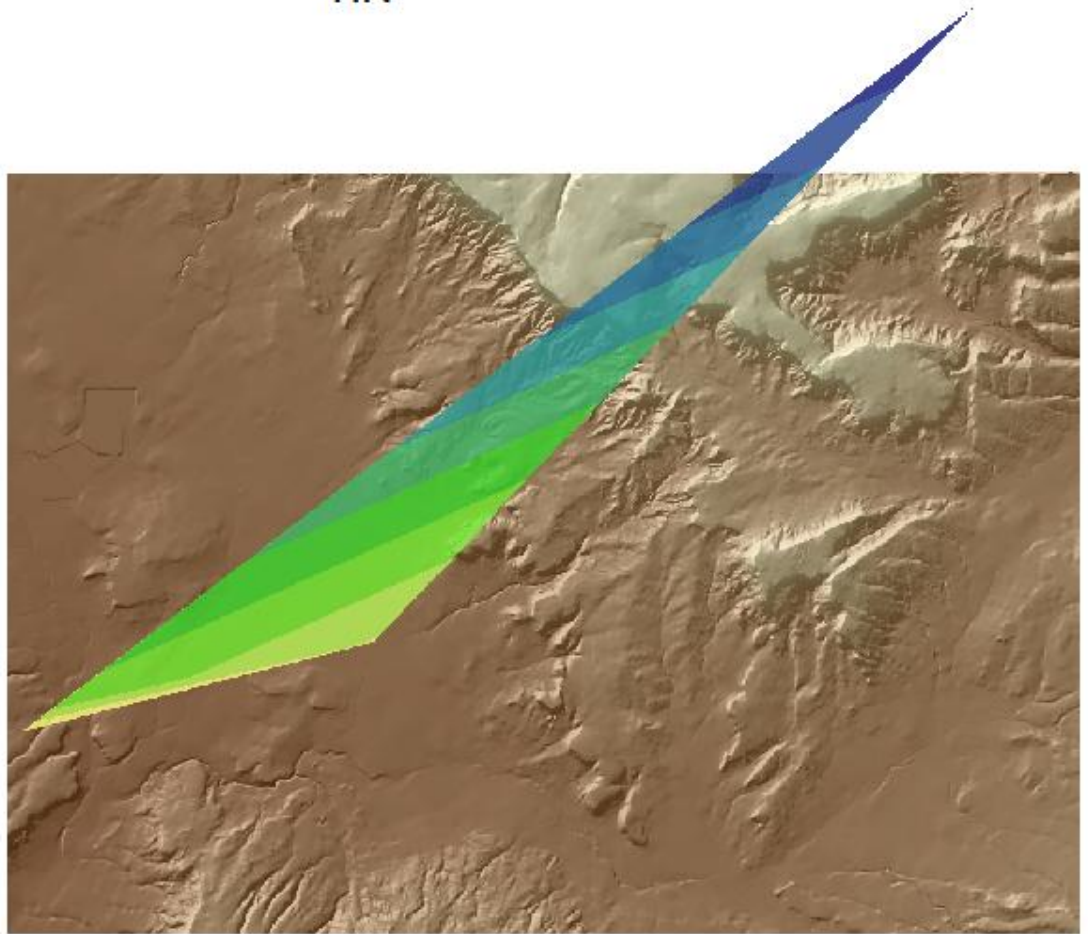
Below the Km aquifer lies the Gallup (Kg) unit however because only one data point for this aquifer exists, no Kriging or TIN is possible.

Below the Kg formation is the Cretaceous Dakota formation (Kd), the data for this formation is confined to the north-central portion of the study area and the TIN for this data suggests a flow direction of NNW to NWN, however only a few data points existed for this formation and this is probably not the most accurate representation of this aquifer.

Kd Water Level Elevations (ft) TIN

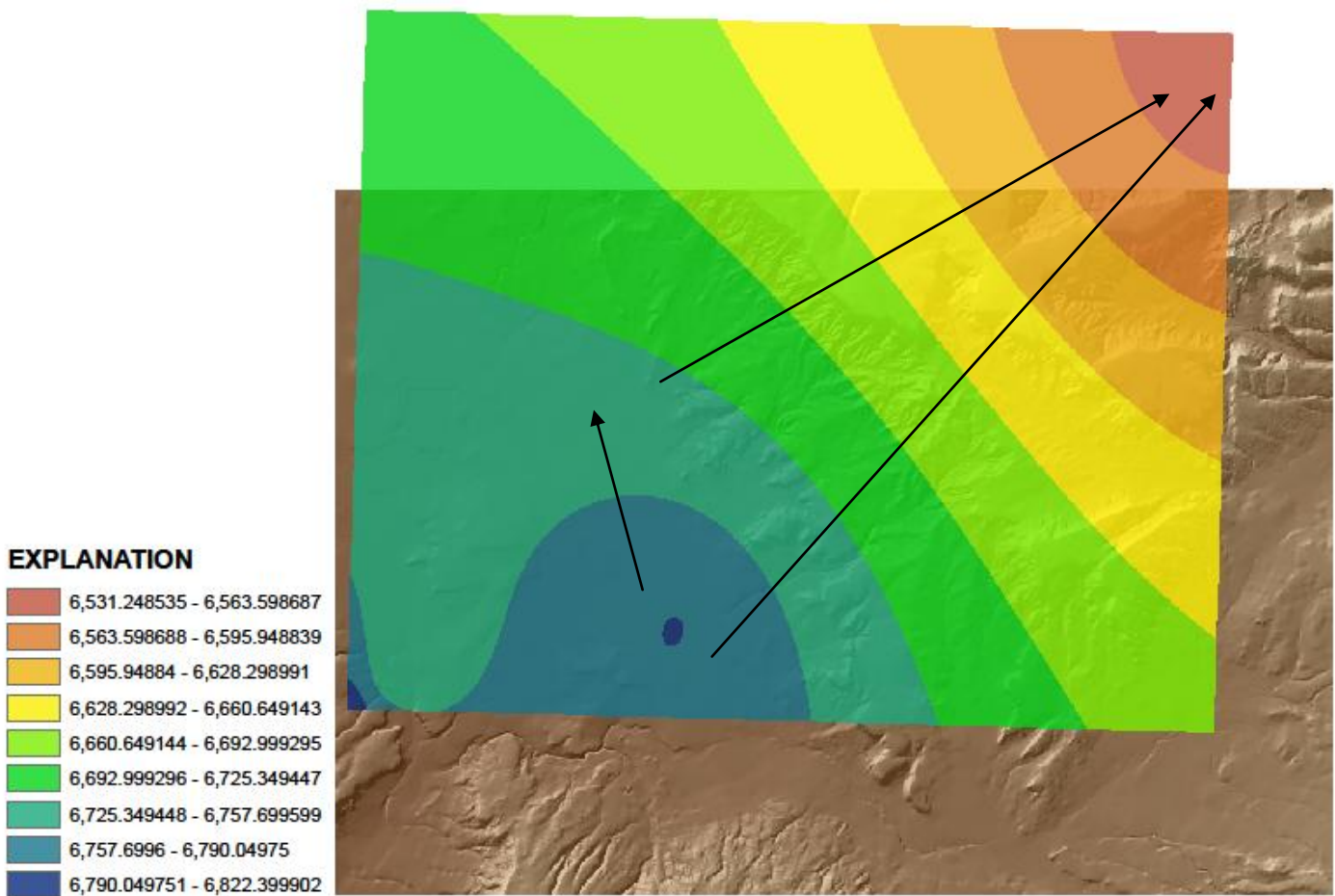
EXPLANATION

6790.022 - 6822.4
6757.644 - 6790.022
6725.267 - 6757.644
6692.889 - 6725.267
6660.511 - 6692.889
6628.133 - 6660.511
6595.756 - 6628.133
6563.378 - 6595.756
6531 - 6563.378



Further ambiguity arises when the Kriging analysis is examined, where general flow patterns are expected to follow the slope down gradient, the TIN Suggests NNW to NWN while the Kriging suggests flows more to the NE. Due to sparse data points for this representation, I would suggest that the Kriging is more accurate as it is spatial correlating function and not a direct path type representation. Trend seems to show that the accuracy of a TIN model breaks down with fewer points compared to a Kriging analysis.

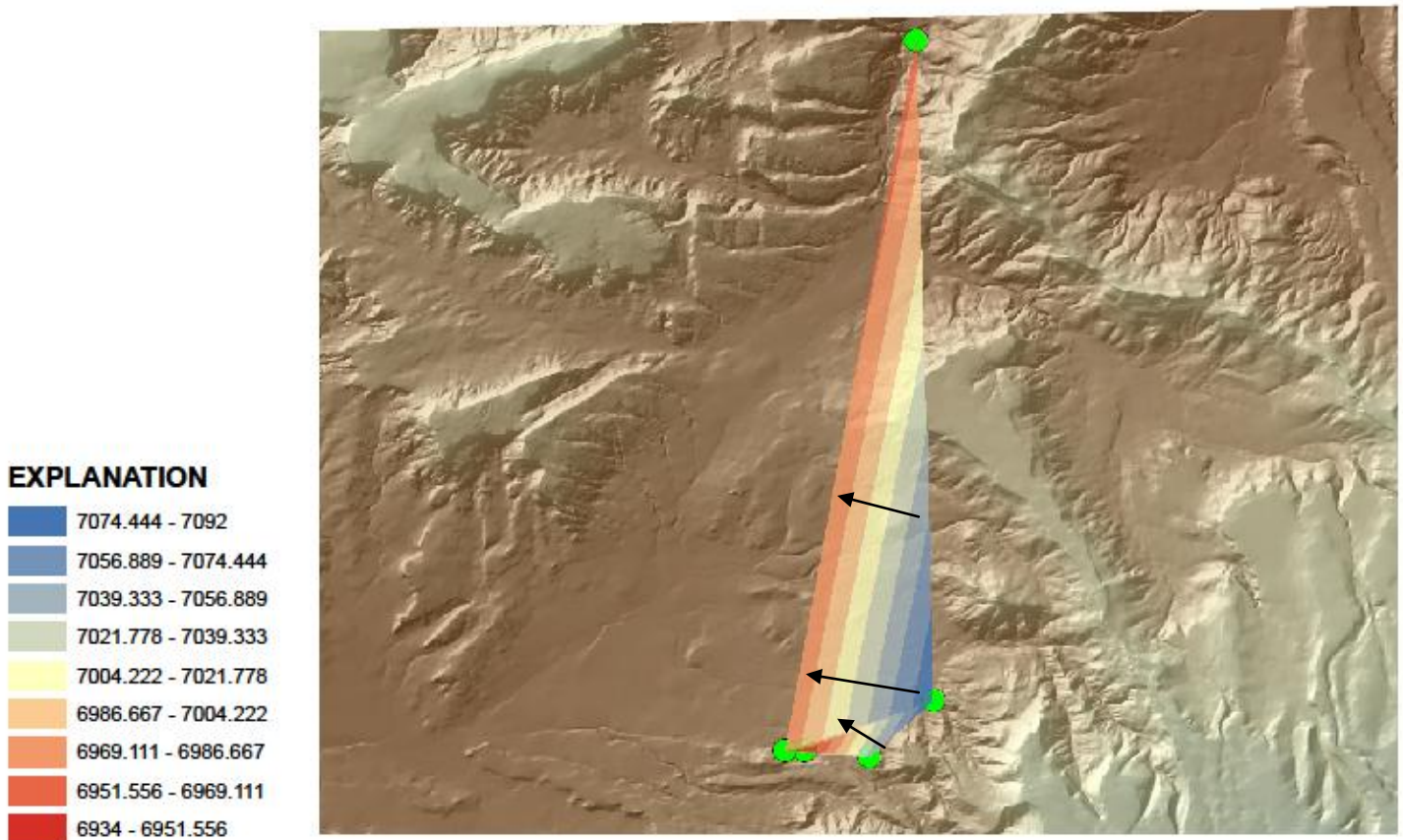
Kd Water Level Elevations (ft)



Should the Kriging be the most accurate, the general down gradient arrows can almost reconcile the suggestions of the TIN for the same data points. The Kriging analysis also generates what is expected for the region and seems to be more accurate than the TIN model.

Below the Kd aquifer is the Kcda formation however the small sum of data for this unit does not allow an analysis either by Kriging or TIN models. Beneath the Kcda is the Cretaceous Point Lookout Sandstone formation, or Kpl.

Kpl TIN



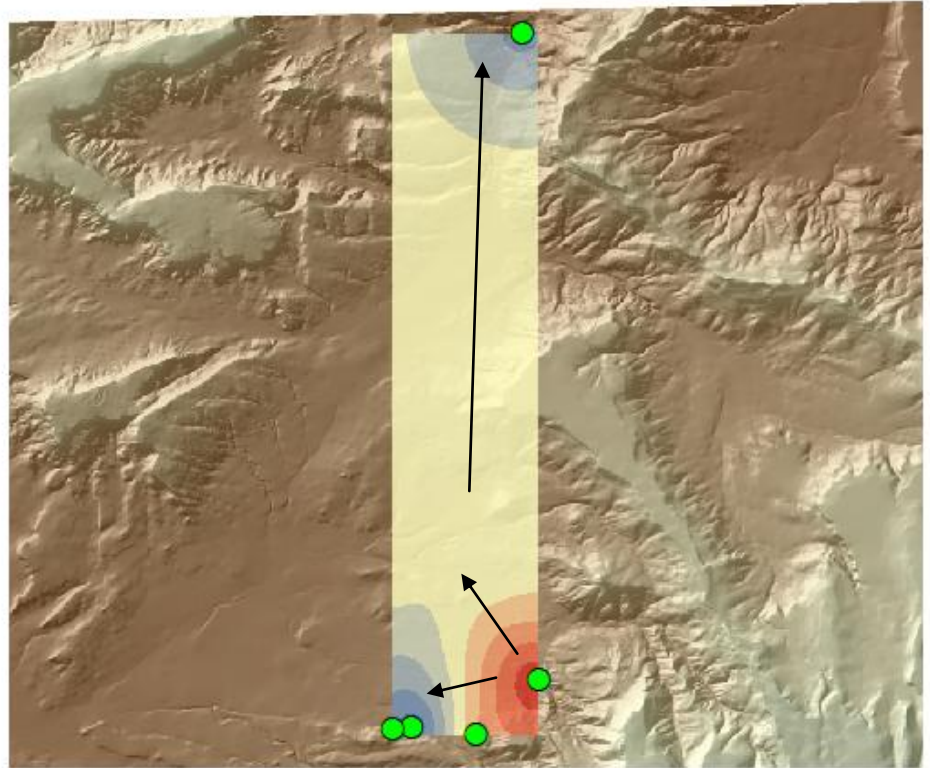
The TIN model for this formation suggests a down slope to the west of the basin, this is most likely due structure of Mt. Taylor bounding the East and South. However analyzing the Kriging can also be beneficial as there are still only very few data points to generate an aquifer surface representation.

Because there are only 5 locations for this data, a TIN is less reliable than a Kriging analysis, again, the image created through Kriging analysis supports the general concept of the San Mateo Hydrology Report with flow directions following the Qal and San Mateo creek to the West as well as a drainage to the north. Examination of the topography and geology of the area where data for this formation is present can also reconcile the differences between the two water surface models. Where flow is generally away from the base of Mount Taylor and would flow north however is bounded by a mesa in the local vicinity (southern portion of data). Because the single point on the NE corner of the Kriging analysis is also a lower elevation the general trend of drainage to the NE is still supported, as well as some drainage through the San Mateo Basin.

Kpl Kriging

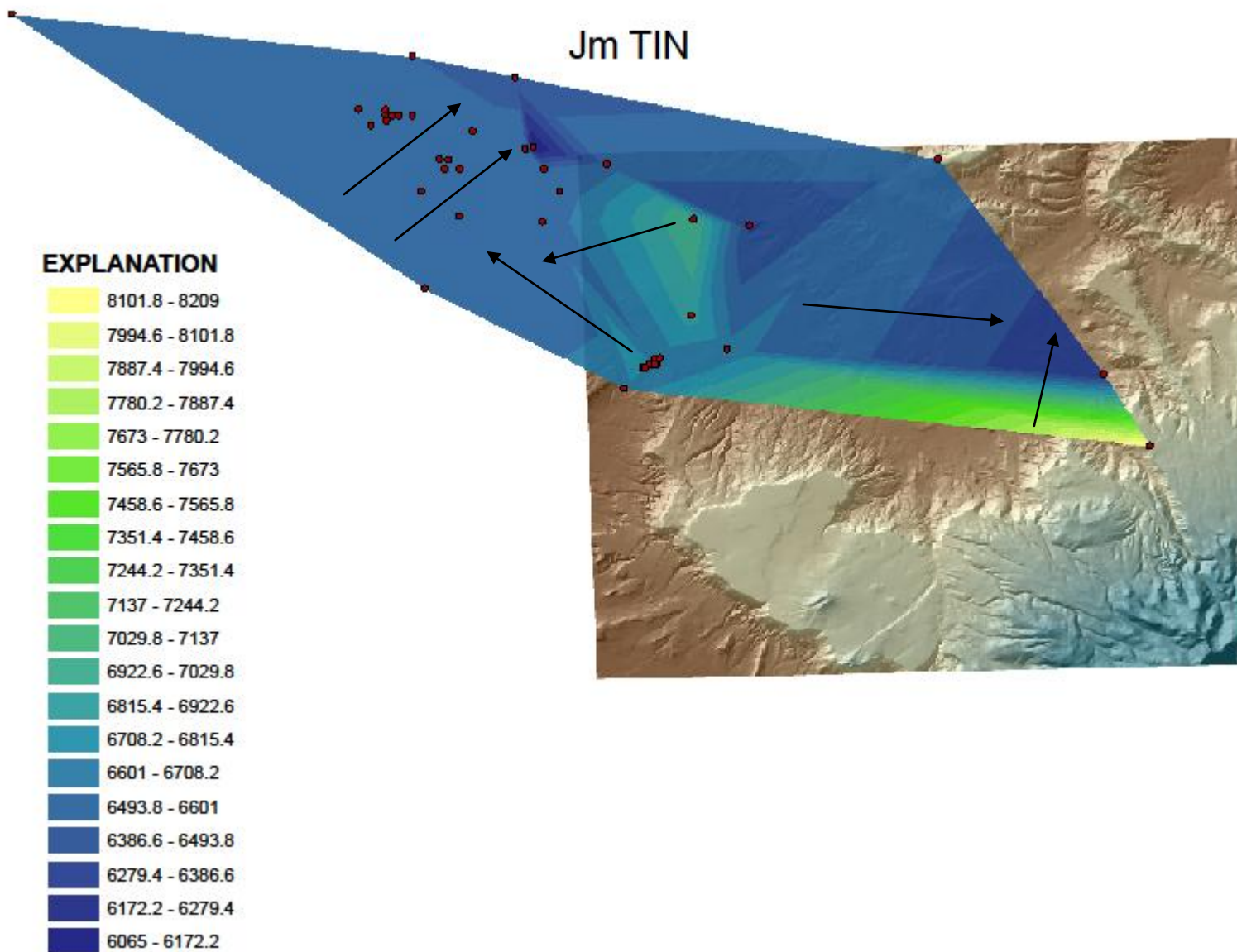
EXPLANATION

	6,942.94043 - 6,958.997776
	6,958.997777 - 6,975.055122
	6,975.055123 - 6,991.112467
	6,991.112468 - 7,007.169813
	7,007.169814 - 7,023.227159
	7,023.22716 - 7,039.284505
	7,039.284506 - 7,055.341851
	7,055.341852 - 7,071.399197
	7,071.399198 - 7,087.456543

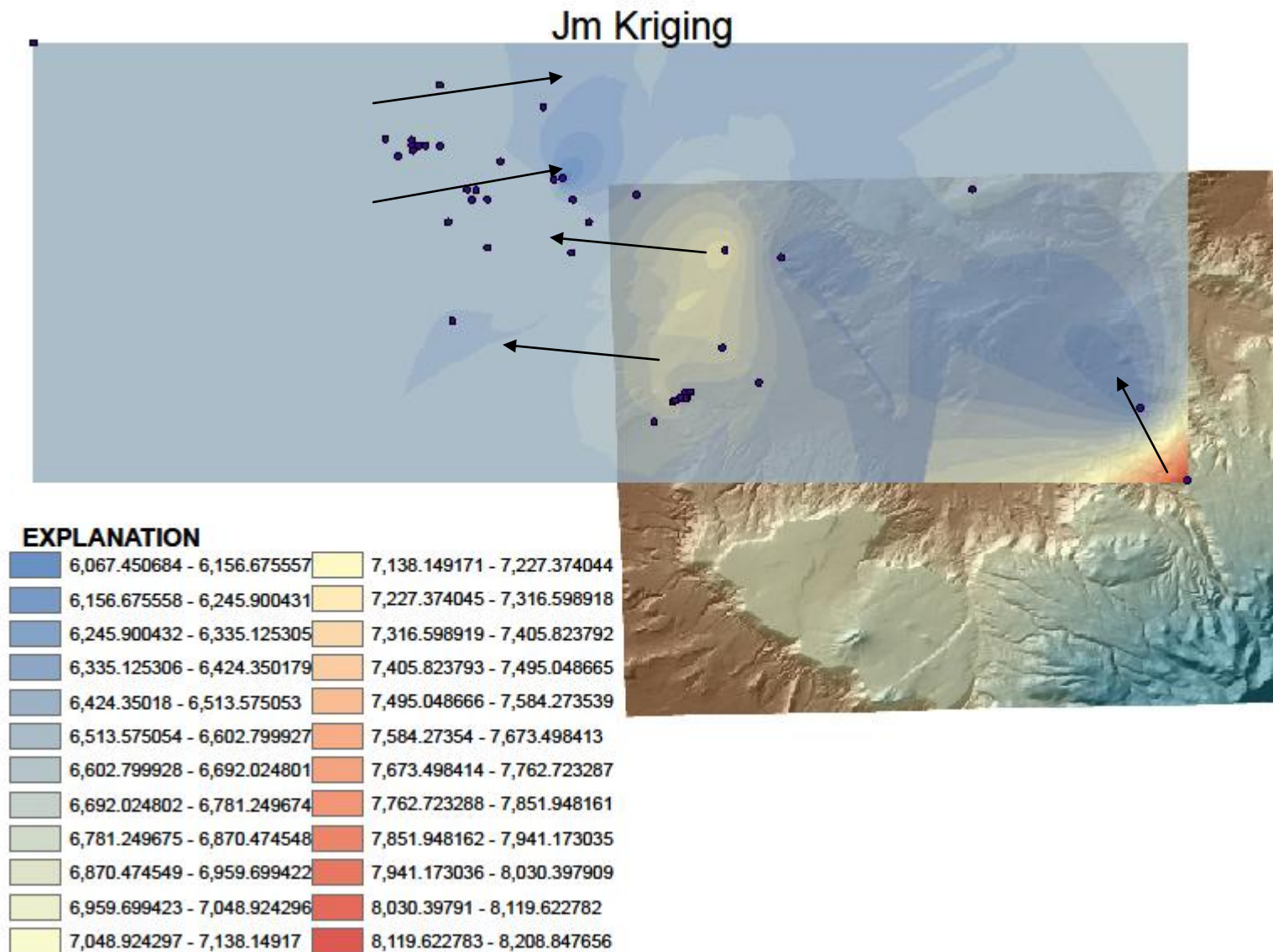


The Point Lookout is the lowest Cretaceous aquifer; beneath the Kpl is the Jurassic Morison formation, (Jm).

This data is a little harder to interpret; several data points allow a good constraint on what is normal however a complex surface occurs without suggesting any outliers.



After examining the down gradient arrows, the down slope trend to the NE still is possible however there are a few data points suggesting a spike in elevation north of the west end of La Jara Mesa. This area was extensively de-watered during heavy Uranium mining activity in the past and this could be causing local deviations in the potentiometric surface levels. The area in the west of the TIN shows several wells with very similar data, it is possible that these wells are mine related and have decreased the SW portion of the aquifers surface level enough to cause a reversal of flow. Water that would have moved NE is not able to due to lower aquifer levels. If this region was previously +/- 200 ft it would drain to the NE almost in its entirety. Another possibility is that a local recharge along a fault or other structure feature acting as a conduit is elevating the surface of this aquifer just south of San Mateo Mesa. This hypothesis is roughly supported by Figure 8 in the Cibola Forest Uranium report, which shows faults in the region of the elevated aquifer surface. This could also potentially be a mixing location.



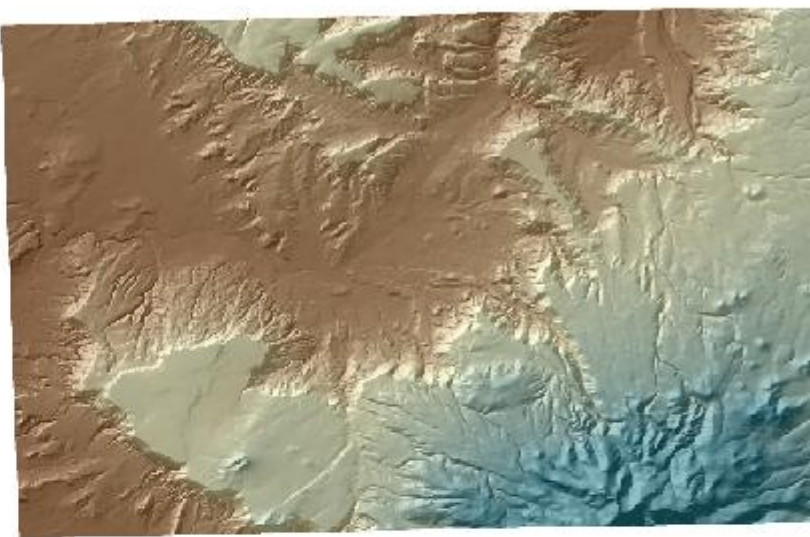
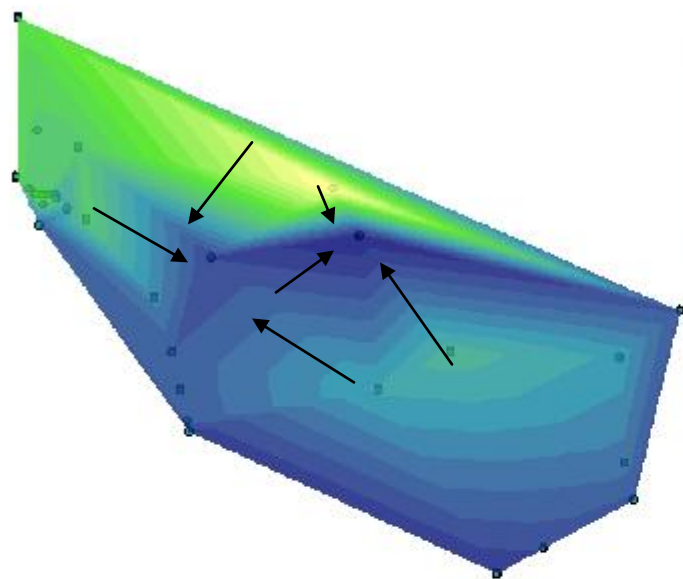
The large quantity of data points for this aquifer cause the Kriging and TIN to be very similar in evaluation of down slope arrows, the main difference occurring in the eastern portion of the models where the data is sparser. Still, the results seem to agree with the Cibola Forest Uranium expectations.

The Jurassic Entrada Sandstone (Je) formation is below the Jm aquifer however due to complicating issues it is discussed at the end of this report.

Below the Je formation is the TRc or Triassic Chinle formation and its aquifer, which lies entirely to the West of the study area. The Tin suggests that this formation dips in the center very similar to the contours of the surface elevation along San Mateo Creek. This could be due to dewatering in the mining region or structure related.

The down gradient arrows show a convergence at the lowest point in the center of the TIN however the data can also be evaluated with the Kriging to show a slight conflict in representation.

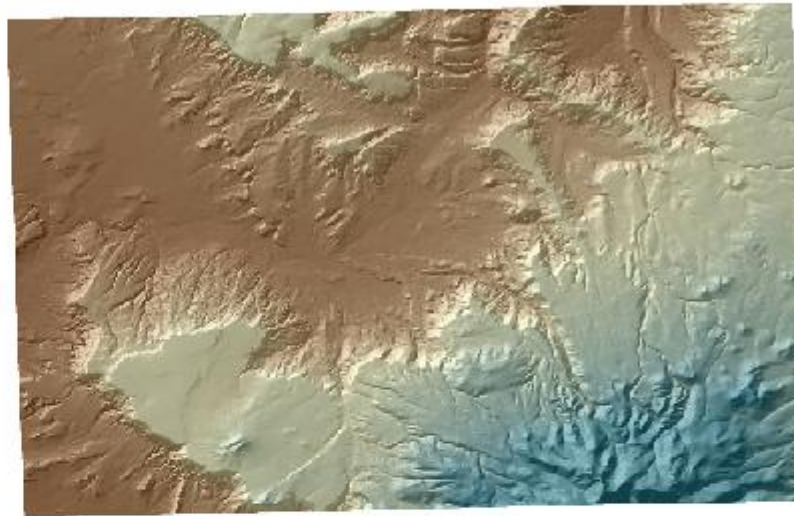
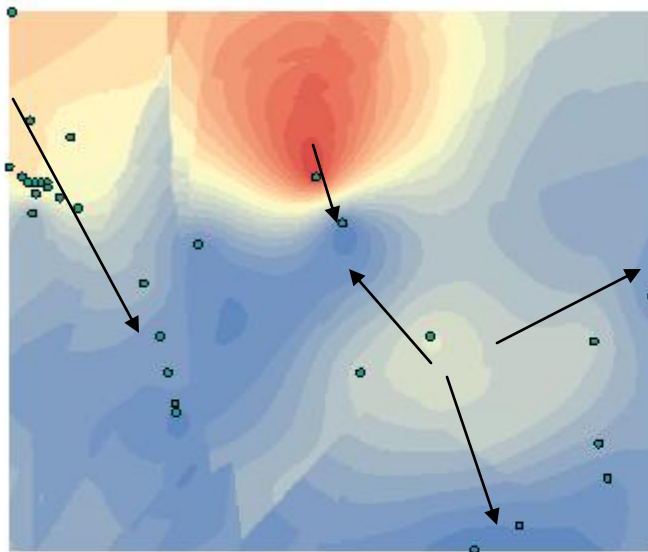
TRc TIN



EXPLANATION

6965.55 - 6993	6691.05 - 6718.5
6938.1 - 6965.55	6663.6 - 6691.05
6910.65 - 6938.1	6636.15 - 6663.6
6883.2 - 6910.65	6608.7 - 6636.15
6855.75 - 6883.2	6581.25 - 6608.7
6828.3 - 6855.75	6553.8 - 6581.25
6800.85 - 6828.3	6526.35 - 6553.8
6773.4 - 6800.85	6498.9 - 6526.35
6745.95 - 6773.4	6471.45 - 6498.9
6718.5 - 6745.95	6444 - 6471.45

TRc Kriging



EXPLANATION

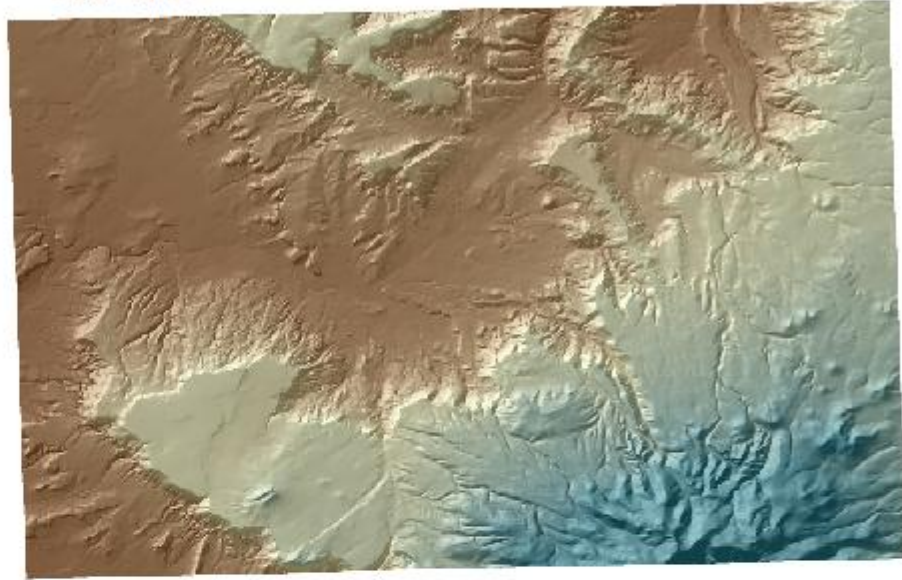
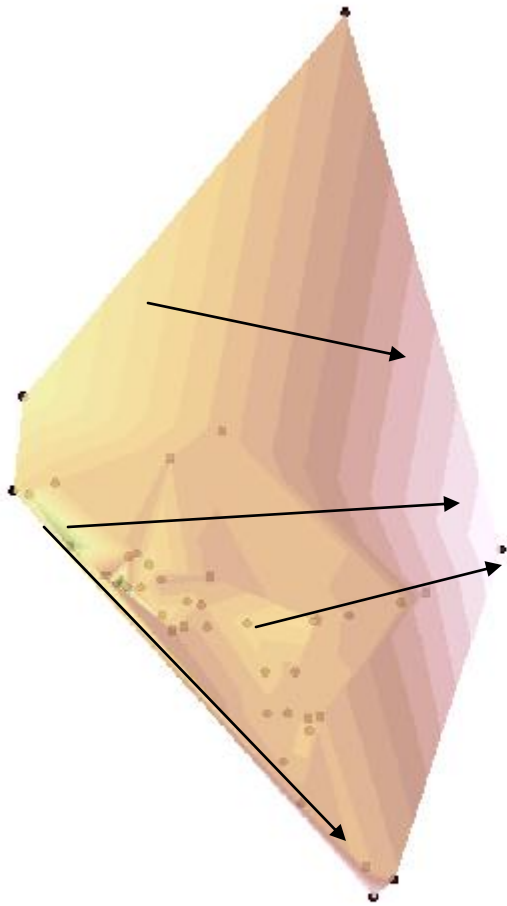
6,478.813477 - 6,502.455835	6,715.237062 - 6,738.879419
6,502.455836 - 6,526.098193	6,738.87942 - 6,762.521777
6,526.098194 - 6,549.740552	6,762.521778 - 6,786.164136
6,549.740553 - 6,573.38291	6,786.164137 - 6,809.806494
6,573.382911 - 6,597.025269	6,809.806495 - 6,833.448853
6,597.02527 - 6,620.667627	6,833.448854 - 6,857.091211
6,620.667628 - 6,644.309985	6,857.091212 - 6,880.733569
6,644.309986 - 6,667.952344	6,880.73357 - 6,904.375928
6,667.952345 - 6,691.594702	6,904.375929 - 6,928.018286
6,691.594703 - 6,715.237061	6,928.018287 - 6,951.660645

The Kriging analysis of this data shows again converging flow paths however still allows for the NE portion to be draining to the NE, the remaining evaluated portions seem to converge and/o flow SW out of the basin.

This data will be presented again with the Je data for a comparison as to which formation the TRw belongs to. As there are only a few points in either the Je or the TRw the TRc is little effected by the addition of the TRw data. Still some knowledge may be gained from the comparison of the two possibilities.

Below the TRc is the Permian San Andreas formation, or Psa, and its aquifer.

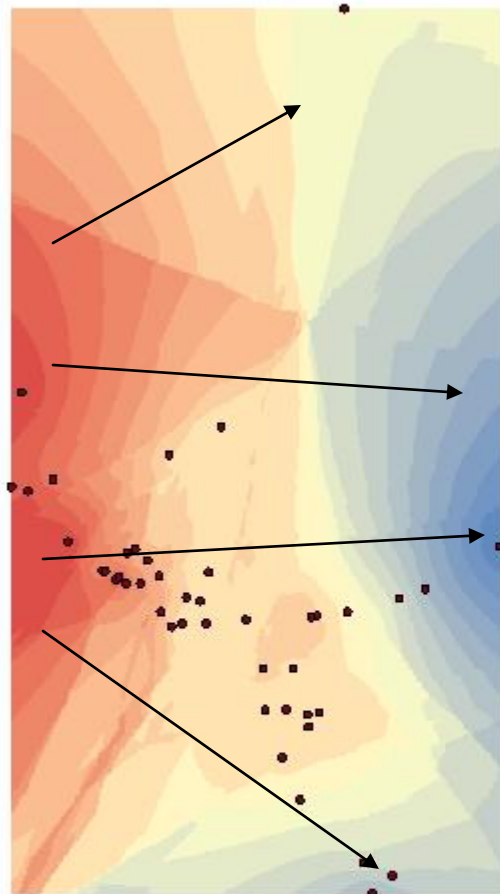
Psa TIN



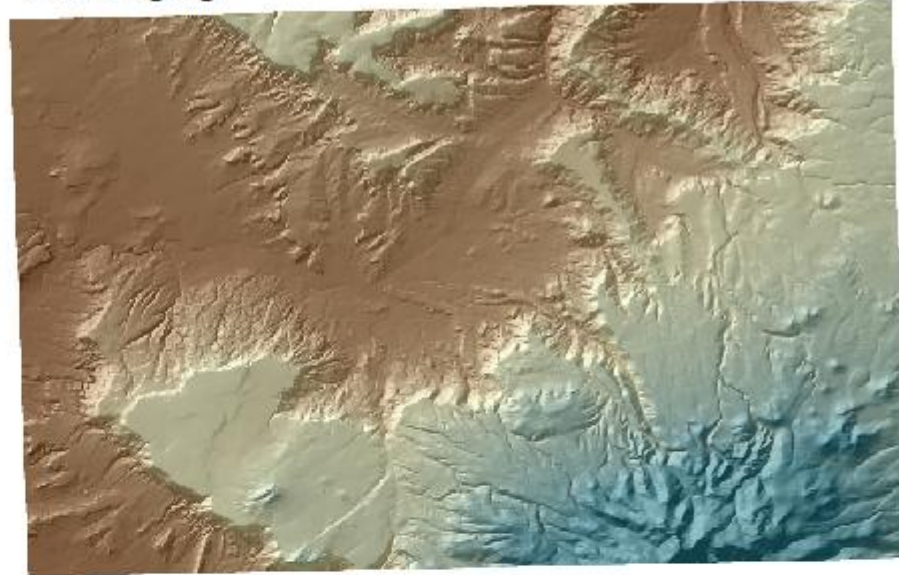
EXPLANATION

6544.4 - 6553	6458.4 - 6467
6535.8 - 6544.4	6449.8 - 6458.4
6527.2 - 6535.8	6441.2 - 6449.8
6518.6 - 6527.2	6432.6 - 6441.2
6510 - 6518.6	6424 - 6432.6
6501.4 - 6510	6415.4 - 6424
6492.8 - 6501.4	6406.8 - 6415.4
6484.2 - 6492.8	6398.2 - 6406.8
6475.6 - 6484.2	6389.6 - 6398.2
6467 - 6475.6	6381 - 6389.6

This data generally suggests that the aquifer slopes to the NE however some complexities are seen in the SW region.



Psa Kriging



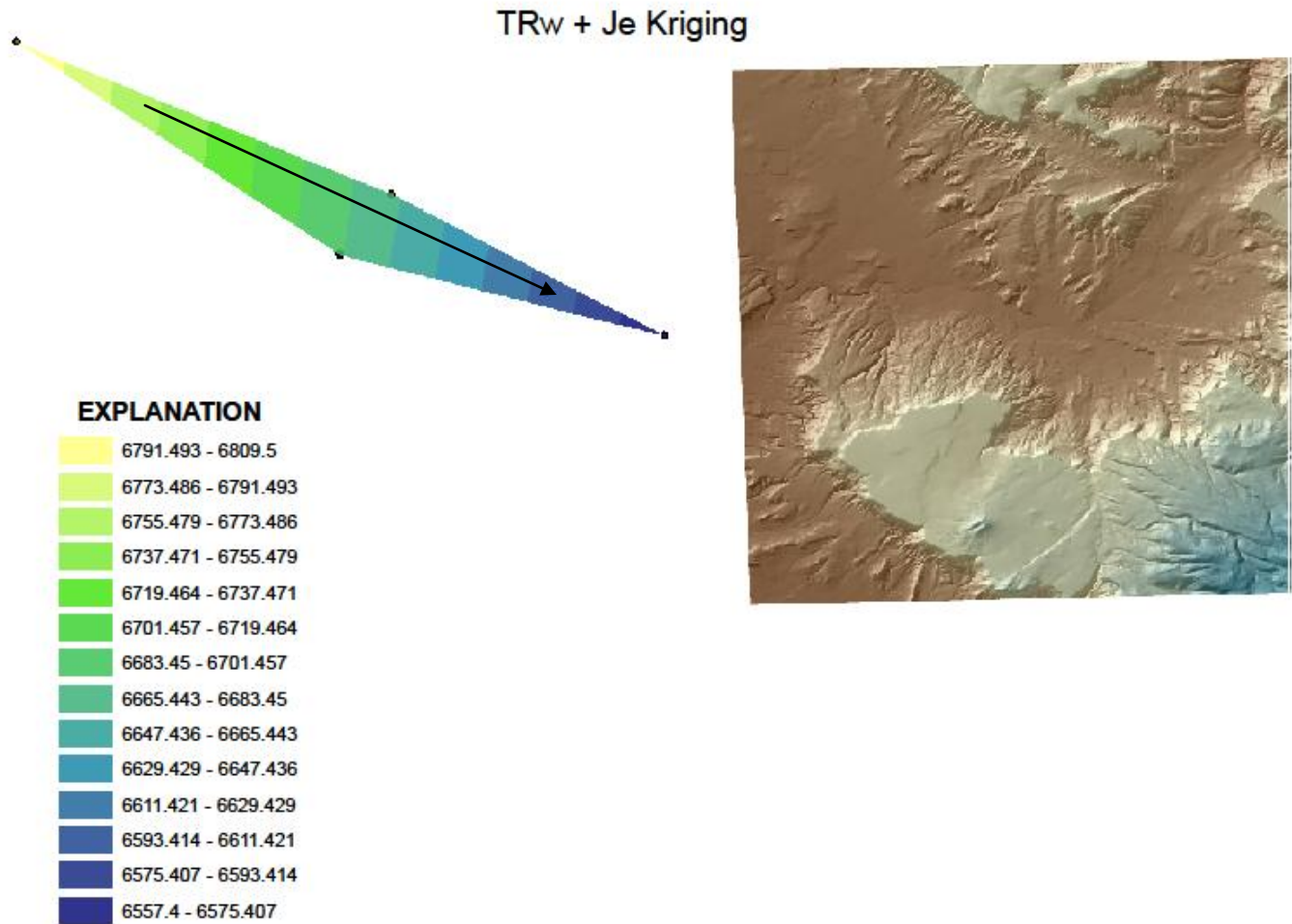
EXPLANATION

6,398.510742 - 6,403.428223	6,447.685548 - 6,452.603027
6,403.428224 - 6,408.345703	6,452.603028 - 6,457.520508
6,408.345704 - 6,413.263184	6,457.520509 - 6,462.437988
6,413.263185 - 6,418.180664	6,462.437989 - 6,467.355469
6,418.180665 - 6,423.098145	6,467.35547 - 6,472.272949
6,423.098146 - 6,428.015625	6,472.27295 - 6,477.19043
6,428.015626 - 6,432.933105	6,477.190431 - 6,482.10791
6,432.933106 - 6,437.850586	6,482.107911 - 6,487.025391
6,437.850587 - 6,442.768066	6,487.025392 - 6,491.942871
6,442.768067 - 6,447.685547	6,491.942872 - 6,496.860352

The Kriging again supports the NE trend of down slope of the aquifer surface and therefore flow direction to the NE is preserved. The Kriging seems to simplify the complexities in the SW region however suggests that the southern portion of the aquifer diverts south and the northern portion diverts north along its eastward flow.

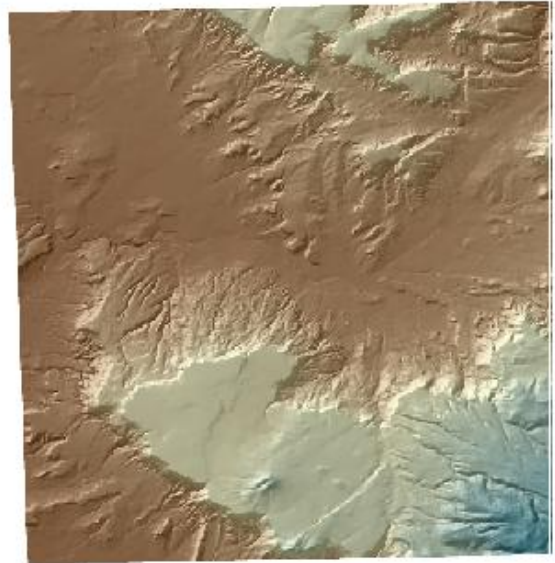
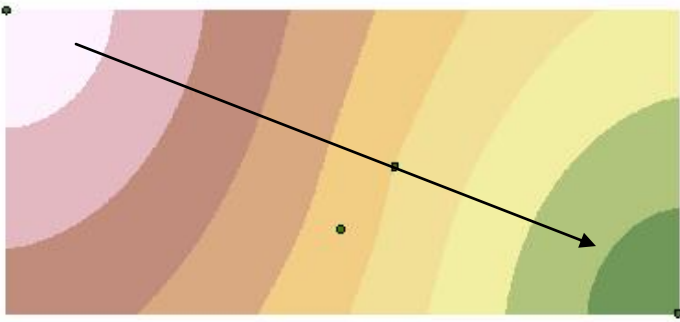
The overall suggestions of both of these models agree very well.

The Data for the Je was very sparse however we may be able to add the TRw data to it depending on fit, the combinations of the different possibilities are presented below.








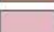



Should we add the TRw data to the Je data this is what is represented, and flow is to the SE however there is still few data and the TIN may not be accurate. Still, analysis of the Kriging yields the same results, flow to the SE generally

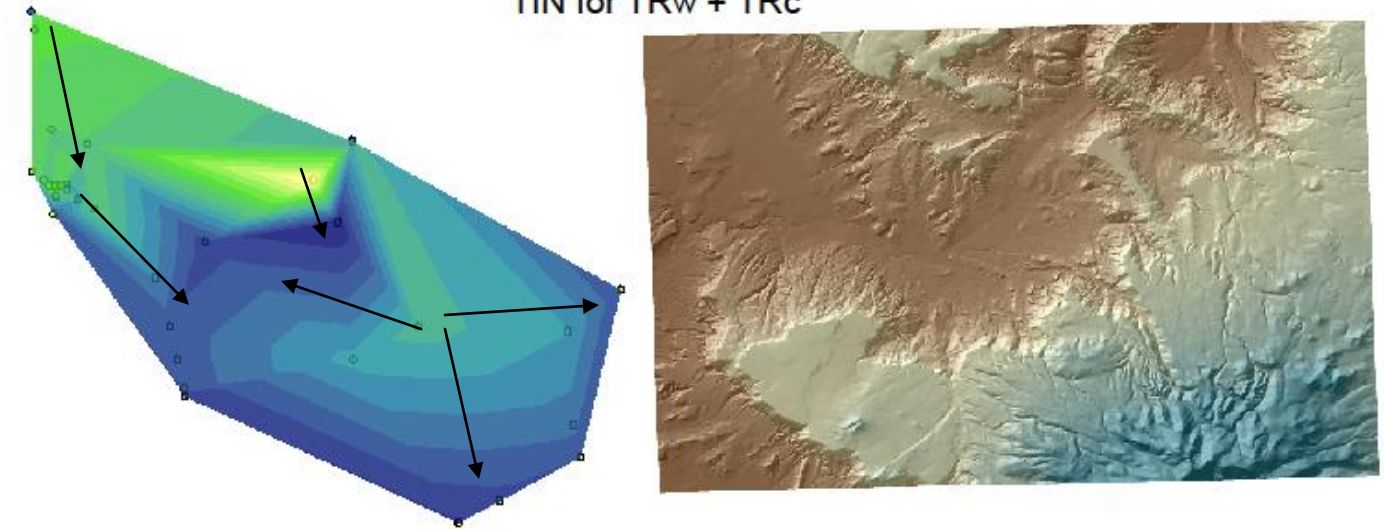
TRw + Je Kriging



EXPLANATION

	6,557.507813 - 6,585.506944
	6,585.506945 - 6,613.506076
	6,613.506077 - 6,641.505208
	6,641.505209 - 6,669.50434
	6,669.504341 - 6,697.503472
	6,697.503473 - 6,725.502604
	6,725.502605 - 6,753.501736
	6,753.501737 - 6,781.500868
	6,781.500869 - 6,809.5

TIN for TRw + TRc

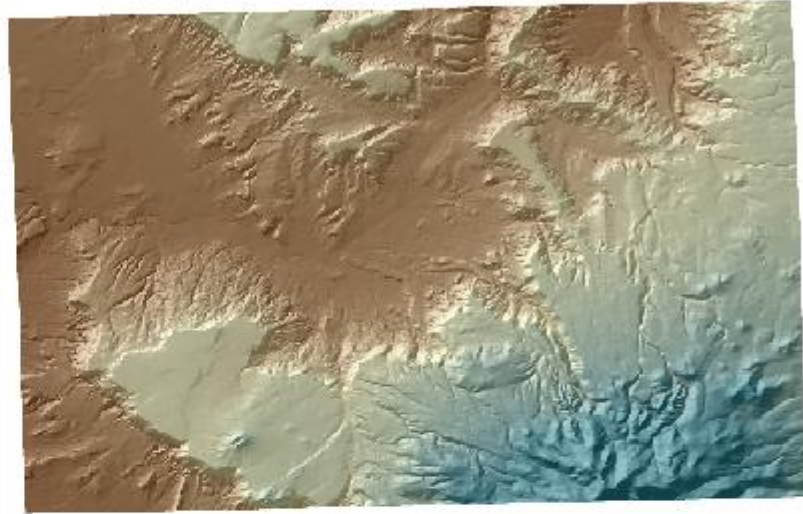
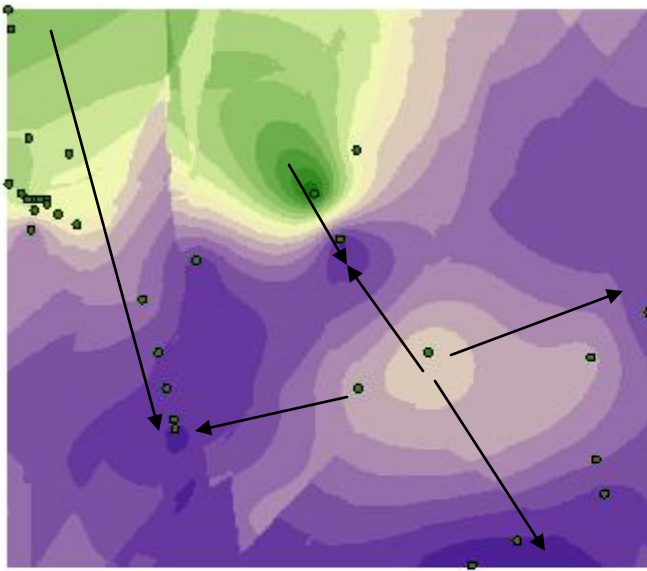


EXPLANATION

6956.4 - 6993	6663.6 - 6700.2
6919.8 - 6956.4	6627 - 6663.6
6883.2 - 6919.8	6590.4 - 6627
6846.6 - 6883.2	6553.8 - 6590.4
6810 - 6846.6	6517.2 - 6553.8
6773.4 - 6810	6480.6 - 6517.2
6736.8 - 6773.4	6444 - 6480.6
6700.2 - 6736.8	

The TIN and Kriging for adding the TRw to the TRc is very similar to the TRc previously viewed however because there are only two data points for the TRw it would not affect the TRc very much. This is evident when evaluating the down slope arrows as well.

TRw + TRc Kriging

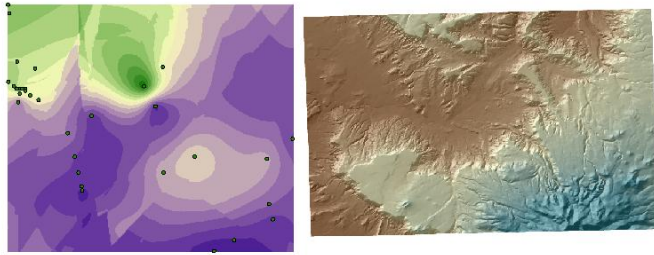


EXPLANATION

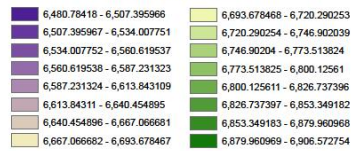
6,480.78418 - 6,507.395966	6,693.678468 - 6,720.290253
6,507.395967 - 6,534.007751	6,720.290254 - 6,746.902039
6,534.007752 - 6,560.619537	6,746.90204 - 6,773.513824
6,560.619538 - 6,587.231323	6,773.513825 - 6,800.12561
6,587.231324 - 6,613.843109	6,800.125611 - 6,826.737396
6,613.84311 - 6,640.454895	6,826.737397 - 6,853.349182
6,640.454896 - 6,667.066681	6,853.349183 - 6,879.960968
6,667.066682 - 6,693.678467	6,879.960969 - 6,906.572754

The TRc + TRw did not seem to fit as well as the TRw + Je however due to lack of data neither the Je nor TRw would be able to be analyzed via TIN modeling or Kriging methods. This leaves the accuracy a bit ambiguous for the Je and TRw however the quantity of TRc data generally causes the models to be unaltered with the addition of TRw, both of these scenarios have a possibility to be correct or incorrect, below is a comparison on the same page for review.

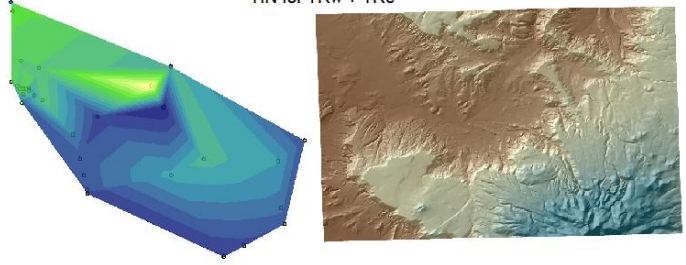
TRw + TRc Kriging



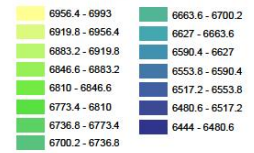
EXPLANATION



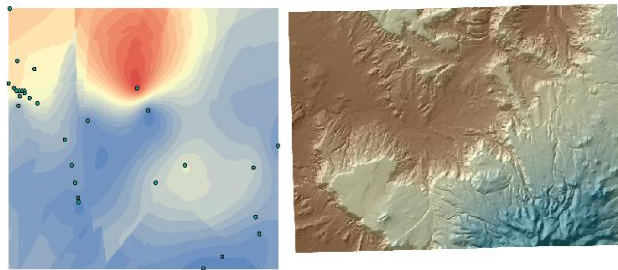
TIN for TRw + TRc



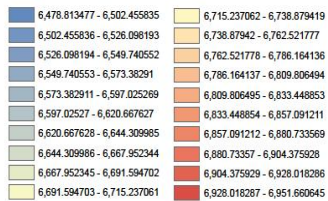
EXPLANATION



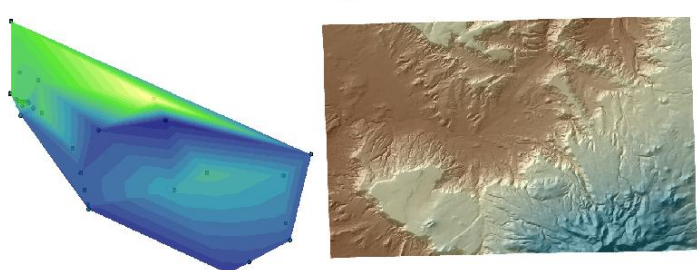
TRc Kriging



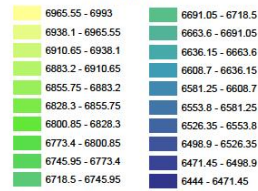
EXPLANATION

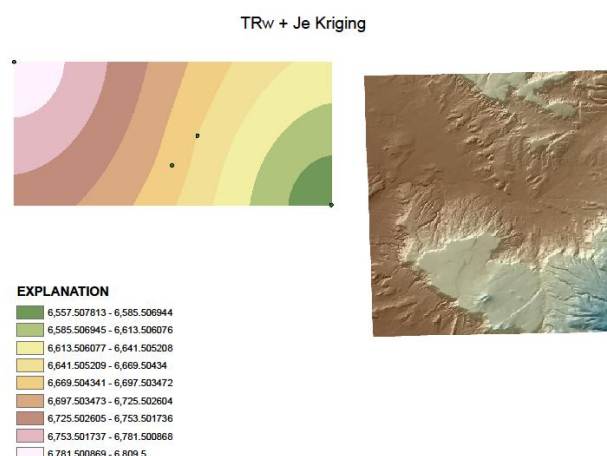
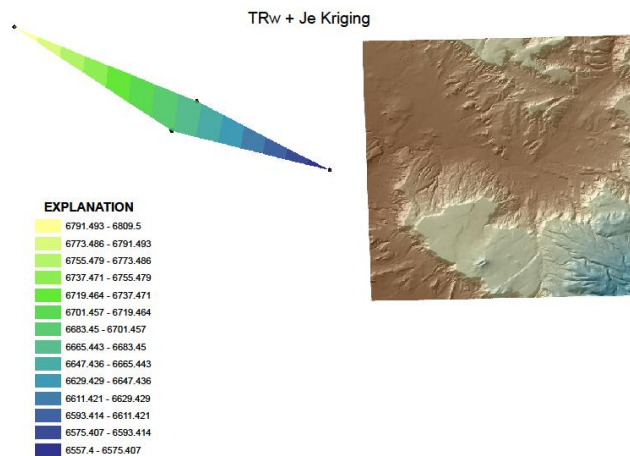


TRc TIN



EXPLANATION





Neither the Je nor the TRw can be analyzed on their own for comparison to original models.

Qal Data				
	LAT_DD	LONG_DD	ELEV	Formation
	35.1602778	-107.8275000	6417.0	Qal
	35.1602778	-107.8275000	6429.0	Qal
	35.1602778	-107.8211111	6437.0	Qal
	35.2097222	-107.8561111	6468.0	Qal
	35.2102778	-107.8891667	6462.0	Qal
	35.2036111	-107.8877778	6483.0	Qal
	35.1850000	-107.8980556	6450.0	Qal
	35.1869444	-107.8855556	6450.0	Qal
	35.1750000	-107.8905556	6450.0	Qal
	35.1705556	-107.8891667	6467.0	Qal
	35.1688889	-107.8733333	6800.0	Qal
	35.1675000	-107.8866667	6452.0	Qal
	35.1597222	-107.8388889	6429.0	Qal
	35.1525000	-107.8647222	6436.0	Qal
	35.1525000	-107.8647222	6431.0	Qal
	35.1491667	-107.8566667	6435.0	Qal
	35.2961111	-107.8311111	6599.0	Qal
	35.2775000	-107.8302778	6582.0	Qal
	35.2766667	-107.8436111	6567.0	Qal
	35.2463889	-107.8713889	6520.0	Qal
	35.2402778	-107.8725000	6485.0	Qal
	35.2327778	-107.9108333	6453.0	Qal
	35.2427778	-107.9238889	6462.0	Qal
	35.2316667	-107.9136111	6480.0	Qal
	35.2733333	-107.9813889	6550.0	Qal
	35.3327778	-107.6608333	7276.0	Qal
	35.3469444	-107.7366667	6853.4	Qal
	35.3226940	-107.6843430	7062.0	Qal
	35.3339800	-107.5672830	7122.0	Qal
	35.3466520	-107.7755500	6797.0	Qal
	35.3477330	-107.7383810	6856.0	Qal
	35.3481020	-107.7389960	6856.0	Qal
	35.3635810	-107.7692070	6863.0	Qal
	35.3300050	-107.6433730	7352.0	Qal
	35.3300050	-107.6433730	7352.0	Qal
21	35.3226940	-107.6843430	7062.0	Qal
33	35.3339800	-107.5672830	7122.0	Qal
87	35.3300050	-107.6433730	7352.0	Qal
106	35.3635810	-107.7692070	6863.0	Qal
28	35.336645	-107.654352	7144.0	Qal
40	35.343529	-107.637220	7274.0	Qal
43	35.342350	-107.637197	7277.0	Qal
44	35.342350	-107.637197	7277.0	Qal
53	35.338606	-107.637206	7303.0	Qal
54	35.335986	-107.637079	7310.0	Qal
55	35.338611	-107.637153	7303.0	Qal
59	35.332627	-107.637154	7362.0	Qal
60	35.332627	-107.637154	7362.0	Qal
69	35.338493	-107.635434	7326.0	Qal
70	35.336026	-107.635632	7326.0	Qal
76	35.330493	-107.643860	7233.5	Qal
79	35.331210	-107.644511	7267.5	Qal
88	35.330909	-107.653146	7181.8	Qal
115	35.346646	-107.775566	6746.0	Qal
119	35.345595	-107.756427	6816.5	Qal
120	5.347722	-107.738361	6833.0	Qal
121	35.348102	-107.738996	6833.0	Qal

Kmf				
Well#	LAT_DD	LONG_DD	ELEV	Formation
	35.354167	-107.646389	7108.5	Kmf
	35.343889	-107.664444	7073.0	Kmf
	35.336389	-107.651111	7142.0	Kmf
	35.345278	-107.630556	7189.0	Kmf
	35.335278	-107.642500	7240.0	Kmf
	35.335278	-107.642500	7210.0	Kmf
	35.334444	-107.641667	7205.0	Kmf
	35.330833	-107.641944	7274.0	Kmf
	35.332500	-107.652778	7182.0	Kmf
	35.368383	-107.658814	7121.0	Kmf
	35.335482	-107.657170	7055.0	Kmf
	35.333911	-107.642986	7209.0	Kmf
	35.319818	-107.693012	7050.0	Kmf
100	35.319818	-107.693012	7050.0	Kmf
7	35.352677	-107.646304	7074.2	Kmf
27	35.335544	-107.657158	7137.5	Kmf
39	35.345767	-107.640204	7257.0	Kmf
41	35.342223	-107.640142	7202.0	Kmf
42	35.342276	-107.640204	7198.0	Kmf
45	35.339816	-107.637132	7290.0	Kmf
46	35.339816	-107.637132	7290.0	Kmf
48	35.343504	-107.631216	7323.0	Kmf
56	35.332548	-107.641623	7297.0	Kmf
57	35.332584	-107.641627	7297.0	Kmf
58	35.334797	-107.637139	7316.0	Kmf
61	35.332603	-107.641631	7196.0	Kmf
62	35.333837	-107.642967	7233.3	Kmf
63	35.334808	-107.640152	7141.0	Kmf
64	35.334799	-107.637043	7301.0	Kmf
65	35.334796	-107.637141	7316.0	Kmf
75	35.331334	-107.641771	7260.0	Kmf
80	35.328713	-107.641681	7312.0	Kmf
89	35.334202	-107.653033	7179.0	Kmf
92	35.331243	-107.645870	7255.5	Kmf
107	35.360193	-107.750375	6799.1	Kmf
133	35.418362	-107.634682	6967.1	Kmf
	35.384272	-107.637006	7159.0	Kmf
5	35.384272	-107.637006	7159.0	Kmf
83	35.331685	-107.640401	7044.0	Kmf
123	35.432673	-107.607250	6913.0	Kmf
127	35.455961	-107.634141	6972.0	Kmf

Km				
LAT	LONG	ELEV	Formation	Well#
35.338559	-107.632607	6652	Km	67
35.338622	-107.632689	6649	Km	72
35.440979	-107.663362	6701	Km	128
35.433735	-107.670991	7247	Km	130

Kd				
Well #	LAT_DD	LONG_DD	ELEV	Formation
	35.361389	-107.750278	6792.1	Kd
	35.353056	-107.796389	6734.1	Kd
	35.349167	-107.802500	6822.4	Kd
129	35.440815	-107.663408	6531.00	Kd

Kpl				
Well #	LAT_DD	LONG_DD	ELEV	Formation
	35.332500	-107.648333	6934	Kpl
	35.331701	-107.640431	7044.0	Kpl
66	35.338559	-107.632607	7092.00	Kpl
90	35.332425	-107.650665	6974.00	Kpl
132	35.418362	-107.634682	6963.97	Kpl

Jm				
	LAT_DD	LONG_DD	ELEV	Formation
	35.415833	-107.853333	6545	Jmw
	35.343889	-107.631389	6276	Jmw
	35.348889	-107.781389	6616.3	Jmw
	35.339167	-107.791667	6643.3	Jmw
	35.347222	-107.782778	6625.2	Jmw
	35.347222	-107.780556	6636.5	Jmw
	35.372500	-107.858056	6508	Jmw
	35.443056	-107.828056	6456	Jmw
	35.414167	-107.797500	6540.6	Jmw
	35.412500	-107.818333	6520	Jmw
	35.419167	-107.824722	6541	Jmw
	35.419722	-107.821944	6065	Jmw
	35.405000	-107.813056	6529	Jmw
	35.395000	-107.818889	6512.6	Jmw
	35.450278	-107.862222	6600	Jmw
	35.432500	-107.880278	6552	Jmw
	35.426944	-107.876111	6573.8	Jmw
	35.432222	-107.871389	6551	Jmw
	35.430278	-107.871389	6549	Jmw
	35.428611	-107.871111	6547	Jmw

	35.430278	-107.869167	6549	Jmw
	35.430278	-107.866944	6548	Jmw
	35.430278	-107.862222	6547	Jmw
	35.430278	-107.862222	6543	Jmw
	35.430278	-107.862222	6546	Jmw
	35.425000	-107.842222	6531	Jmw
	35.415833	-107.853333	6550	Jmw
	35.415833	-107.853333	6549	Jmw
	35.415833	-107.853333	6549	Jmw
	35.415833	-107.686667	6549	Jmw
	35.415556	-107.850278	6546	Jmw
	35.412500	-107.851667	6541	Jmw
	35.412500	-107.846667	6541	Jmw
	35.412500	-107.846667	6539	Jmw
	35.396667	-107.846667	6539	Jmw
	35.405000	-107.859444	6549	Jmw
	35.464167	-107.996111	6587.1	Jmw
	35.349190	-107.779605	6643.0	Jmw
	35.450278	-107.862222	6495	Jmr
	35.352222	-107.757222	6625	Jm
	35.363581	-107.769207	6863.0	Jmw
111	35.349190	-107.779605	6643.0	Jmw
1	35.319931	-107.615916	8209.00	Jmw
110	35.347139	-107.781227	6613.30	Jmw
112	35.346006	-107.785522	6831.00	Jmw
113	35.347063	-107.783189	6742.00	Jmw
114	35.346215	-107.784570	6739.00	Jmw
134	35.393436	-107.749718	6369.70	Jmw
135	35.395801	-107.768387	7034.00	Jmw

Je			
LAT_DD	LONG_DD	ELEV	Formation
35.357222	-107.936111	6685	Je
35.330556	-107.828889	6557	Jt

TRc			
LAT_DD	LONG_DD	ELEV	Formation
35.268056	-107.834167	6567	TRc
35.304167	-107.836111	6629	TRc
35.293056	-107.918333	6641	TRc
35.255833	-107.831111	6519	TRc
35.239167	-107.862222	6503	TRc
35.230556	-107.878056	6476	TRc
35.293056	-107.986111	6533	TRc
35.282222	-107.983611	6532	TRc
35.278889	-107.983056	6480	TRc
35.320000	-107.815556	6522	TRc
35.305833	-107.893611	6680.4	TRc
35.381667	-108.034722	6744.7	TRc
35.381667	-108.034722	6735	TRc
35.365556	-108.041944	6757.6	TRc
35.376111	-108.020556	6733.8	TRc
35.360000	-108.033056	6709.8	TRc
35.360000	-108.033056	6820.1	TRc
35.360000	-108.028611	6656	TRc
35.356111	-108.032778	6710.8	TRc
35.349167	-108.033889	6539	TRc
35.354722	-108.024444	6720.2	TRc
35.354722	-108.024444	6653	TRc
35.338333	-107.975556	6496	TRc
35.324444	-107.994722	6593.8	TRc
35.305833	-107.988889	6528.2	TRc
35.420000	-108.041111	6786.8	TRc
35.345833	-107.924722	6444	TRcpc
35.361944	-107.933889	6993	TRcps
35.360000	-108.030833	6741	TRcs
35.358333	-108.028333	6734.8	TRcs
35.351111	-108.017778	6685	TRcs
35.351111	-108.017778	6730	TRcs
35.361944	-108.037500	6731.5	TRcs
35.360000	-108.035278	6812.4	TRcs

TRw			
LAT_DD	LONG_DD	ELEV	Formation
35.377222	-107.918889	6669	TRw
35.426944	-108.042222	6809.5	TRw

Psa			
LAT_DD	LONG_DD	ELEV	Formation
35.217500	-107.905278	6464	Psa
35.217500	-107.895833	6454	Psa
35.204444	-107.904722	6454	Psa
35.204444	-107.898056	6450	Psa
35.203056	-107.891389	6455	Psa
35.199167	-107.891111	6467	Psa
35.203611	-107.887778	6451	Psa
35.189444	-107.899444	6465	Psa
35.189444	-107.899444	6455	Psa
35.176111	-107.893889	6443	Psa
35.152500	-107.864722	6443	Psa
35.156389	-107.873611	6452	Psa
35.146944	-107.871111	6385	Psa
35.293333	-107.918611	6454	Psa
35.284444	-107.935000	6458	Psa
35.247778	-107.922500	6446	Psa
35.255833	-107.831111	6381	Psa
35.242500	-107.854444	6410	Psa
35.239444	-107.862500	6448	Psa
35.233889	-107.888611	6453	Psa
35.235278	-107.878889	6449	Psa
35.233611	-107.890278	6479	Psa
35.232778	-107.910833	6453	Psa
35.232778	-107.910833	6472	Psa
35.246389	-107.938056	6447	Psa
35.235278	-107.937500	6474	Psa
35.239722	-107.929444	6465	Psa
35.238611	-107.925278	6457	Psa
35.230556	-107.934167	6440	Psa
35.231667	-107.930833	6453	Psa
35.231667	-107.923333	6454	Psa
35.304167	-107.981389	6510	Psa
35.276944	-107.971389	6466	Psa
35.274444	-107.984444	6475	Psa
35.273333	-107.979167	6510	Psa
35.257222	-107.966667	6534	Psa
35.255000	-107.945556	6457	Psa
35.248056	-107.955833	6438	Psa
35.248056	-107.955000	6435	Psa
35.253611	-107.948056	6451	Psa
35.251389	-107.941667	6480	Psa
35.245278	-107.951667	6553	Psa
35.246111	-107.950556	6547	Psa
35.244167	-107.948333	6453	Psa
35.244167	-107.943889	6473	Psa
35.424722	-107.880000	6442.3	Psa

